Nature's Carbonylation Catalyst: Raman Spectroscopic Evidence That Carbon Monoxide Binds to Iron, Not Nickel, in CO Dehydrogenase

Di Qiu, Manoj Kumar, Stephen W. Ragsdale,* Thomas G. Spiro*

Carbon monoxide dehydrogenase catalyzes the synthesis of acetyl–coenzyme A from coenzyme A, a methyl group, and carbon monoxide. The carbon monoxide binds to a mixed metal center of the enzyme, which contains nickel bridged to an iron-sulfur cluster. Resonance Raman spectroscopy has been used to identify both C-O stretching and metal-CO stretching vibrations of the carbon monoxide adduct of the enzyme. This adduct was shown by isotopic exchange to be on the pathway for acetyl–coenzyme A synthesis. The metal to which carbon monoxide is bound was established to be iron, not nickel, by preparation of enzyme from bacteria grown on iron-54 and nickel-64. The Fe-CO frequency is low, 360 wave numbers, implying a weak bond, probably because of electron donation from sulfide and thiolate ligands of the iron. A bimetallic mechanism is proposed, in which carbon monoxide binds to an iron atom and is subsequently attacked by a methyl group on a nearby nickel atom, forming an acetyl ligand, which is then transferred to coenzyme A.

Carbon monoxide dehydrogenase (CODH) is a CO-metabolizing enzyme of anaerobic autotrophic bacteria (*1*). It catalyzes two types of reactions with CO that bear intriguing analogies to industrial CO chemistry of great commercial importance. On the one hand, CO is oxidized to CO_2 at an iron-containing center, providing reducing equivalents to the enzyme (*2, 3*). This reaction is analogous to the industrial production of H_2 by the water-gas shift reaction: $CO + H_2O = CO_2 + H_2$ (*4*). CODH can also reduce CO_2 to CO, and in contrast to known electrocatalytic systems, a negligible overpotential is required (*5*). The activation of CO_2 implied by this observation is important in exploiting this abundant compound in synthetic reactions. In another type of carbonylation chemistry, CODH catalyzes the combination of CO with a methyl group to produce the acetyl group of acetyl–coenzyme A (acetyl-CoA). This reaction is analogous to acetic acid production by the carbonylation of methanol (*6*) and is related to the wider arena of industrial carbonylation chemistry (*7*), in which hydrocarbons and their oxygenates are built up from CO and H_2. All of these industrial processes are carried out with transition metal catalysts; CODH contains nickel and iron, and these metals are known to be at the enzyme active sites (*1*). The industrial processes generally require elevated pressure and temperature, whereas the enzyme operates under ambient conditions. An understanding of the enzyme mechanism may therefore contain important lessons for the efficient conversion of carbon feedstocks to synthetic fuels and other organic molecules. Because nickel is an uncommon element in biology, it has been the prime candidate as the site of binding and assembly of the acetyl constituents, CO, and a methyl group. Using resonance Raman (RR) spectroscopy, we have discovered, however, that the site of CO binding is not Ni, but rather an Fe atom.

The CODH from *Clostridium thermoaceticum* contains 2 Ni and 11 to 15 Fe atoms (*8*) arranged in three centers—namely, A, B, and C—that can be distinguished by electron paramagnetic resonance (EPR) spectroscopy. Cluster A contains one Ni and three to four Fe atoms (the EPR spectrum is sensitive to Ni as well as Fe isotopes), probably in a Ni-X-Fe_4S_4 structure (*5, 9, 10*). Center B is an ordinary $(Fe_4S_4)^{2+}$ or $(Fe_4S_4)^{+}$ cluster (*9, 10*), whereas center C is an Fe-containing cluster of unknown composition (*5, 9*). Center A is directly involved in acetyl-CoA synthesis; the CO adduct has been shown by infrared (IR) spectroscopy to serve as a precursor of the carbonyl group of acetyl-CoA (*11*). Center C, on the other hand, is implicated in CO oxidation, because this reaction is strongly inhibited by cyanide (*8, 12*), which binds to center C (*2*). By using stopped flow kinetics and freeze-quench EPR spectroscopy, Kumar *et al.* (*3*) have recently shown that CO binds first to center C, where it is oxidized to CO_2. The electrons derived from this oxidation are transferred first to center B and then to center A, which then binds CO and incorporates it into acetyl-CoA.

In the absence of CoA or of methyl donors, CO is bound to center A in a stable CO adduct. The CO stretching frequency $\Delta\nu$ of this adduct is 1995 cm^{-1}, shifting to 1950 cm^{-1} upon ^{13}CO substitution (*11*). When acetyl-CoA is added to the ^{13}CO adduct, isotope exchange is observed in the IR spectrum, with about one-fourth of the CO signal appearing at the ^{12}CO position (*11*). This experiment established that the CO adduct of center A is a catalytically relevant intermediate in the enzymatic pathway. The same result is observed in the RR spectrum, obtained by laser excitation at 476.5 nm (Fig. 1). When ^{13}CO-containing enzyme is incubated with natural abundance acetyl-CoA, RR bands are observed at 1993 and 1950 cm^{-1}, with a ~1:3 intensity ratio. Thus, the C-O stretching mode of the exchange-competent CO adduct is enhanced in the RR spectrum.

This adduct also gives rise to a metal-CO stretching mode in the RR spectrum (Fig. 2). A band is seen at 360 cm^{-1}, which shifts to 356 or 353 cm^{-1} upon ^{13}CO or $C^{18}O$ isotope substitution. These shifts are typical of the metal-CO vibration of metal carbonyl complexes (*13*). The 360 cm^{-1} band also demonstrates isotope exchange with acetyl-CoA. Acetyl-CoA addition to ^{13}CO-containing enzyme induces a metal-CO band at the ^{12}CO position (Fig. 1), establishing conclusively that the 360 and

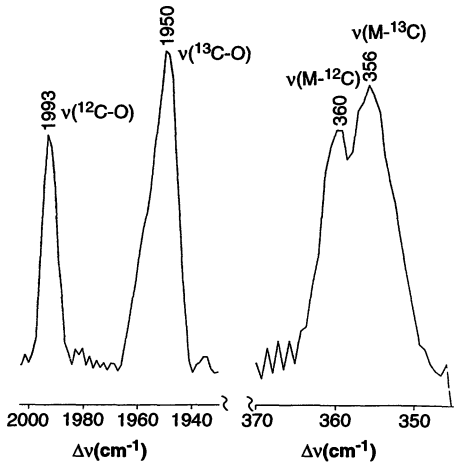

Fig. 1. Resonance Raman bands associated with C-O and M-C stretching, obtained by means of the 476.5-nm Ar^+ laser excitation of the ^{13}CO adduct of CODH in 50 mM tris-maleate buffer (pH 5.5) and 2 mM dithiothreitol that had been incubated with 0.2 mM $CH_3{}^{12}CO$-CoA for 20 min. The finding of adduct bands associated with ^{12}CO as well as ^{13}CO shows the adduct to be in exchange equilibrium with acetyl-CoA. The enzyme was prepared as described in (*8*). The RR spectra were obtained for frozen pellets of enzyme solution on a liquid N_2 cold finger (*23*). The backscattered light was analyzed with a Spex Triplemate spectrograph equipped with a 2400 grooves per millimeter grating and an intensified diode array detector (Princeton Instruments). Laser power at the sample was about 90 mW, and the collection time was ~4 hours per spectrum. The data were smoothed with a Savitsky-Golay routine, and a 358 cm^{-1} band of the buffer was subtracted digitally.

D. Qiu and T. G. Spiro, Department of Chemistry, Princeton University, Princeton, NJ 08544, USA.
M. Kumar and S. W. Ragsdale, Department of Biochemistry, University of Nebraska, Lincoln, NE 86583, USA.

*To whom correspondence should be addressed.

1993 cm^{-1} vibrations arise from the same CO adduct.

To identify the metal to which the CO is bound, we prepared the enzyme from bacteria grown on both ^{54}Fe and ^{64}Ni. The 360 cm^{-1} band shifts to 362 cm^{-1} in the ^{54}Fe-containing enzyme but does not shift at all in the ^{64}Ni-containing enzyme (Fig. 2). For a linear triatomic M-C-O oscillator, the expected isotope shift is 2.0 cm^{-1} for ^{54}Fe and 5.0 cm^{-1} for ^{64}Ni. The observed ^{54}Fe shift is as expected for an Fe-CO adduct, but the undetectable shift upon ^{64}Ni substitution rules out a Ni-CO adduct (the Fe isotope sensitivity was confirmed with ^{57}Fe-containing enzyme, which showed a 1 cm^{-1} downshift and a 3 cm^{-1} difference with respect to the ^{54}Fe-containing enzyme). This surprising result is reminiscent of the recent finding that the Mo atom of nitrogenase probably does not bind N_2; the crystal structure shows the Mo to be coordinatively saturated, whereas several Fe atoms in the MoFe cofactor appear to be coordinatively unsaturated and may serve as the binding site (*14*). In the Fe_4S_4 cluster of center A, the Fe atoms are presumably four-coordinate. The CO binding requires expansion to five-coordinate Fe or displacement of an endogenous ligand.

The 360 cm^{-1} frequency is quite low for Fe-CO stretching and suggests a rather weak Fe-CO bond. By comparison, CO adducts of heme proteins with histidine ligands have Fe-C frequencies near 500 cm^{-1} (with C-O frequencies near 1950 cm^{-1}). When the axial ligand is cysteine, the Fe-C frequency is lowered to ~470 cm^{-1} because thiolate is a stronger donor than imidazole (*13*). Because the Fe atoms in center A are in an Fe-S cluster, it is possible that electron donation by the bridging sulfide and terminal cysteine ligands weakens the Fe-CO bond substantially. Model chemistry for this effect is not currently available. Addition of CO to $[Fe_4S_4(SPh)_4]^{3-}$ was reported (*15*) to generate a ^{13}C-sensitive EPR spectrum, accounting for 5 to 10% of the Fe. Solutions prepared in this way contain a complex mixture of species, however (*16*).

It is surprising that CO bound to an Fe_4S_4 cluster gives rise to RR bands because the electronic transitions in the visible region are Fe-S charge transfer in character (*17*). Moreover, CO binds to the reduced form of center A (*3*), in which the cluster is at the $(Fe_4S_4)^+$ redox level. The RR enhanced Fe-S stretching modes are well cataloged for $(Fe_4S_4)^{2+}$ clusters (*18*), but $(Fe_4S_4)^+$ clusters are notoriously weak scatterers and no RR spectra have been reported (*17*). Oxidized CODH shows several RR bands at expected Fe-S frequencies (*19*), but none are seen in the CO adduct spectrum, consistent with reduction of the cluster. Only the Fe-CO stretching band is enhanced. Evidently the Fe-CO bond distance is significantly altered in the resonant charge transfer excited state. This observation is consistent with the backbonding mechanism of CO binding because the transfer of charge from S to the Fe $d\pi$ orbitals increases the extent of backbonding and should therefore shorten the Fe-CO bond relative to the ground state. It is nevertheless unexpected that the Fe-CO bond displacement is much more pronounced than the Fe-S bond displacements in the resonant excited state, as implied by the weakness of the Fe-S stretches. Conceivably, the Fe-S modes suffer destructive interference from multiple charge transfer transitions (*18*), whereas the Fe-CO mode does not. Excitation profiles could resolve this question; preliminary experiments showed that excitation at 514.5 nm does not produce a detectable signal, whereas at 441.6 nm, a high background was encountered, perhaps because of the onset of fluorescence.

That CO is bound to Fe in the exchange-competent complex implies that the Fe-S cluster of center A is directly involved in the mechanism of CODH catalysis and is not simply an electron transfer agent. The adjacent Ni atom remains an attractive candidate for the site of methyl transfer. A methyl group is transferred to CODH from a methylated corrinoid–iron-sulfur protein (*20*). This methyl group is incorporated into acetyl-CoA when CO and CoA are subsequently added; in the absence of CoA, addition of CO produces acetate, by means of hydrolysis of the acetyl group generated on the enzyme. Thus, the CO and methyl groups must bind at adjacent sites, presumably at the A center. Although the methylation site might be a cysteine sulfur atom (*4*), Lu *et al.* (*20*) present several lines of evidence against this possibility and in favor of a metal site.

We propose a bimetallic mechanism for acetyl-CoA synthesis as a working hypoth-

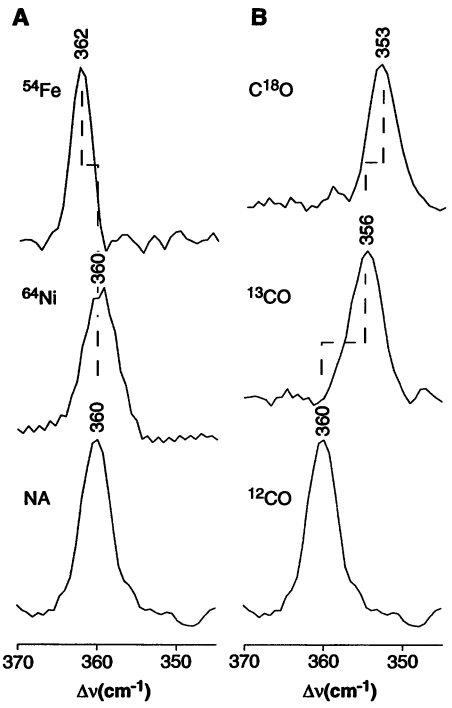

Fig. 2. Resonance Raman band associated with M-C stretching of the CO adduct of CODH. (**A**) The effect of isolating the enzyme from bacteria grown on minimal medium containing ^{64}Ni on the one hand and ^{54}Fe on the other (NA = natural abundance Fe and Ni). (**B**) The effect of replacing $^{12}C^{16}O$ with $^{13}C^{16}O$ and $^{12}C^{18}O$. Conditions as in Fig. 1.

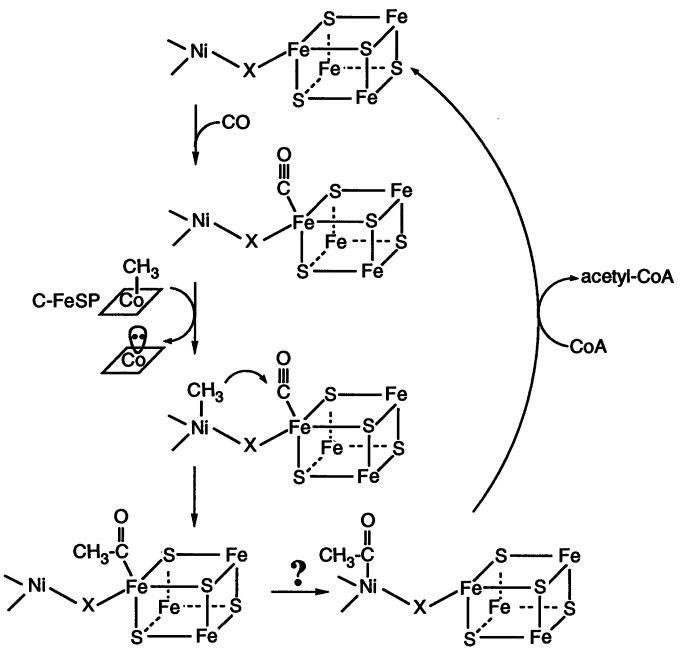

Fig. 3. Working hypothesis for the molecular mechanism of acetyl synthesis at center A of CODH, assuming that Ni is the site of methyl transfer. X, unidentified bridging ligand; C-FeSP, methylated corrinoid–iron-sulfur protein.

esis (Fig. 3). First CO binds at a cluster Fe that is bridged to the Ni. Methyl transfer to the Ni is then followed by attack on the bound CO, forming an acetyl adduct, which might migrate from Fe to Ni. Transfer of the acetyl group to CoA completes the catalytic cycle. Alkyl attack on metal-bound CO is a well-precedented organometallic process that has been extensively studied (*21*). Usually the CO binds to the same metal atom that bears the alkyl group, following dissociation of another ligand. In the mechanism suggested in Fig. 3, the function of the Fe-S cluster is to provide access to CO at ambient temperature and pressure, by way of a binding site that is under redox control. Removal of an electron from a metal center has been found to strongly promote the CO insertion reaction (*22*). Thus, reoxidation of the Fe_4S_4 cluster in center A could accelerate acetyl formation. There is evidence for acceleration of the CO–acetyl-CoA exchange reaction upon addition of one-electron oxidants (*12*).

REFERENCES AND NOTES

1. S. W. Ragsdale, *Crit. Rev. Biochem. Mol. Biol.* **26**, 261 (1991).
2. M. E. Anderson, V. J. DeRose, B. M. Hoffman, P. A. Lindahl, *J. Am. Chem. Soc.* **115**, 12204 (1993).
3. M. Kumar, W.-P. Lu, L. Liu, S. W. Ragsdale, *ibid.*, p. 11646.
4. C. H. Cheng, D. E. Hendrikson, R. Eisenberg, *ibid.* **99**, 2791 (1977).
5. P. A. Lindahl, E. Münck, S. W. Ragsdale, *J. Biol. Chem.* **265**, 3873 (1990).
6. J. W. Roth, J. H. Craddock, A. Hershman, F. E. Pavlik, *Chem. Technol.* **1**, 600 (1971); H. Papp and M. Baerns, in *New Trends in CO Activation*, L. Guczi, Ed. (Elsevier, New York, 1991), pp. 430–460.
7. C. H. Bartholomew, *ibid.*, pp. 158–224.
8. S. W. Ragsdale, J. E. Clark, L. G. Ljungdahl, L. L. Lundie, H. L. Drake, *J. Biol. Chem.* **258**, 2364 (1983).
9. P. A. Lindahl, S. W. Ragsdale, E. Münck, *ibid.* **265**, 3880 (1990).
10. C. Fan, C. M. Gorst, S. W. Ragsdale, B. M. Hoffman, *Biochemistry* **30**, 431 (1991).
11. M. Kumar and S. W. Ragsdale, *J. Am. Chem. Soc.* **114**, 8713 (1992).
12. S. W. Ragsdale and H. G. Wood, *J. Biol. Chem.* **260**, 3970 (1985).
13. X.-Y. Li and T. G. Spiro, *J. Am. Chem. Soc.* **110**, 6024 (1988).
14. M. M. Georgiadis *et al.*, *Science* **257**, 1653 (1992); J. Kim and D. C. Rees, *Nature* **360**, 553 (1992).
15. B. A. Averill and W. H. Orme-Johnson, *J. Am. Chem. Soc.* **100**, 5234 (1978).
16. M. A. Walters and W. H. Orme-Johnson, in *Advances in Nitrogen Fixation Research*, C. Veeger and W. E. Newton, Eds. (Kluwer, Boston, MA, 1984), p. 100.
17. T. G. Spiro, R. S. Czernuszewicz, S. Han, in *Biological Applications of Raman Spectroscopy*, T. G. Spiro, Ed. (Wiley-Interscience, New York, 1988), vol. 3, pp. 523–554.
18. R. S. Czernuszewicz, K. A. Macor, M. K. Johnson, A. Gewirth, T. G. Spiro, *J. Am. Chem. Soc.* **109**, 7178 (1987).
19. D. Qiu, M. Kumar, S. W. Ragsdale, T. G. Spiro, unpublished results.
20. W.-P. Lu, S. R. Harder, S. W. Ragsdale, *J. Biol. Chem.* **265**, 3124 (1990).
21. D. Forster, *Adv. Organomet. Chem.* **17**, 255 (1979).
22. R. H. Magnuson, R. Meirowitz, S. Zulu, W. P. Giering, *J. Am. Chem. Soc.* **104**, 5790 (1982).
23. R. S. Czernuszewicz and M. K. Johnson, *Appl. Spectrosc.* **37**, 297 (1983).

24. We thank J. Schwartz for helpful discussions concerning the mechanistic implications of our results and L. Liu for assistance with protein purification. Supported by grants GM13498 (T.G.S.) from the National Institutes of Health and DE-FG02-91ER20053 (S.W.R.) from the Department of Energy.

20 December 1993; accepted 23 March 1994

Direct Observation of Tube-Like Motion of a Single Polymer Chain

Thomas T. Perkins, Douglas E. Smith, Steven Chu*

Tube-like motion of a single, fluorescently labeled molecule of DNA in an entangled solution of unlabeled lambda-phage DNA molecules was observed by fluorescence microscopy. One end of a 16- to 100-micrometer-long DNA was attached to a 1-micrometer bead and moved with optical tweezers. The molecule was stretched into various conformations having bends, kinks, and loops. As the polymer relaxed, it closely followed a path defined by its initial contour. The relaxation time of the disturbance caused by the bead was roughly 1 second, whereas tube-like motion in small loops persisted for longer than 2 minutes. Tube deformation, constraint release, and excess chain segment diffusion were also observed. These observations provide direct evidence for several key assumptions in the reptation model developed by de Gennes, Edwards, and Doi.

Understanding the behavior of a concentrated solution of flexible polymers is a challenging problem in condensed matter physics. Interactions between entangled polymer chains lead to a rich variety of unusual properties. On long time scales, these materials flow like a viscous liquid; on shorter time scales, they have the elastic response of rubber; and for still shorter times, they display glass-like behavior (*1*). These viscoelastic materials play an important role in many biological systems and have broad commercial applications.

The most popular and successful theoretical model for a concentrated polymer solution is the reptation model of de Gennes, Edwards, and Doi (*2*–*6*). The key assumption of the model is that an entangled polymer chain is confined to an imaginary tube through which it moves in snake-like fashion (Fig. 1). The notion of a tube, originally proposed by Edwards (*3*), is based on the idea that a chain is topologically constrained by its neighbors from undergoing transverse displacements. As a consequence, the chain behaves as if it were trapped in a small tube that follows its own contour. The motion of an individual chain is governed by one-dimensional diffusion within the tube. De Gennes originally modeled this motion as diffusion of a gas of noninteracting defects carrying stored length along the chain. The chain ends can diffuse or "reptate" out of the original tube, creating new portions of tube. He conjectured that the results might extend to the case of concentrated or molten polymers in which the tubes would be effectively frozen on time scales less than the characteristic time separating the viscous from the elastic domain. De Gennes (*4*) and Doi and Edwards (*5*) extended the basic reptation model to include tube deformation and constraint release, which would allow the tube to undergo limited transverse motion on longer time scales. Tube deformation is predicted to occur when a strained polymer relaxes its strain by deforming the surround-

Department of Physics, Stanford University, Stanford, CA 94305, USA.

*To whom correspondence should be addressed.

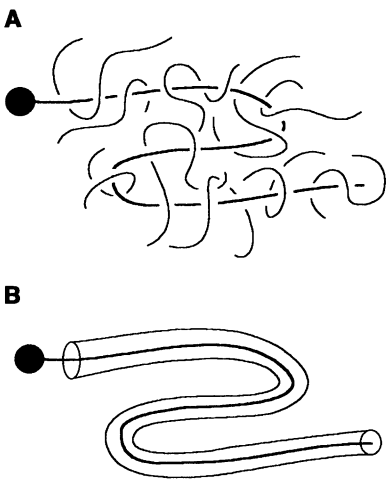

Fig. 1. Schematic representation of the experiment. (**A**) A stained DNA molecule in a concentrated solution of unstained λ-phage DNA was manipulated with optical tweezers by means of a 1.0-μm latex bead attached to one end of the molecule. (**B**) The topological constraints of all the background chains collectively act to confine the polymer to motion within a tube-like region along its own contour.